

4. Masterov V. F., Nasredinov F., Seregin P. P., Huzhakulov E. S., Hajdarov R. A. Parametry tenzora GJEP v uzлах medi i barija reshetki  $\text{La}_{1.9}\text{Ba}_{0.1}\text{CuO}_4$ , opredelennye metodom emissionnoj messbaujerovskoj spektroskopii // Fizika tverdogo tela. 1991. T.3. Vyp. 6. S. 1912–1915.
5. Masterov V. F., Nasredinov F. S., Seregin N. P., Seregin P. P., Saidov Ch. S. Prostranstvennoe raspredelenie dyrok v reshetkah  $\text{RBa}_2\text{Cu}_3\text{O}_7$  // Sverhprovodimost': fizika, himija, tehnologija. 1992. T. 5. Vyp.10. S. 1830–1841.
6. Masterov V. F., Nasredinov F. S., Seregin N. P., Seregin P. P., Davydov A. V., Kumzerov Ju. A. Osobnosti zarjadovogo raspredelenija v reshetke  $\text{PrBa}_2\text{Cu}_3\text{O}_7$  // Fizika tverdogo tela. 1997. T. 39. Vyp. 7. S. 1163–1164.
7. Seregin P. P., Seregin N. P., Masterov V. F., Nasredinov F. S. Effektivnye zarjady atomov v  $\text{YBa}_2\text{Cu}_3\text{O}_7$ , opredelennye metodom emissionnoj messbaujerovskoj spektroskopii // Sverhprovodimost': fizika, himija, tehnologija. 1991. T. 4. Vyp. 6. S. 1136–1143.
8. Seregin P. P., Masterov V. F., Nasredinov F. S., Seregin N. P., Saidov Ch. S. Tensor kristallicheskogo gradienta elektricheskogo polja v uzлах redkozemel'nyh metallov reshetok  $\text{RBa}_2\text{Cu}_3\text{O}_7$  i  $\text{La}_{2-x}\text{Sr}_x\text{CuO}_4$  // Sverhprovodimost': fizika, himija, tehnologija. 1994. T. 7. Vyp. 3. S. 467–474.
9. Bordovsky G., Marchenko A., and Seregin P. Mossbauer of Negative Tcenters in Semiconductors and Superconductors. Identification, Properties, and Applicaton. Academic Publishing GmbH & Co. 2012. 499 p.
10. Tarascon J. M., McKinnon W. R., Greene L. H., Hull G. W., Vogel B. M. Oxygen and rare-earth doping of the 90 K superconducting  $\text{RBa}_2\text{Cu}_3\text{O}_7$ . Phys. Rev. B. 1987. V. 36. P. 226–237; LePage Y., Siegrist T., Sunshine S. A., Schneemeyer L. P., Murphy D. W., Zahurak S. M., Waszczak J.V., McKinnon W. R., Tarascon J. M., Hull G. W., Greene L. H. Neutron diffraction of atomic displacements in  $\text{RBa}_2\text{Cu}_3\text{O}_7$ . Phys. Rev. B. 1987. V. 36. P. 3617–3621.
11. Bordovskii G. A., Marchenko A. V., and Seregin P. P. Atomic Charges in  $\text{YBa}_2\text{Cu}_3\text{O}_7$ ,  $\text{YBa}_2\text{Cu}_4\text{O}_8$ , and  $\text{Y}_2\text{Ba}_4\text{Cu}_7\text{O}_{15}$  Ceramic Samples // Glass Physics and Chemistry 2009. V. 35. Вып. 6. S. 643–651.
12. Wortmann G., and Felner I. Magnetic order of the Pr sublattice in tetragonal and orthorhombic  $\text{Pr}_{1-x}\text{Gd}_x\text{Ba}_2\text{Cu}_3\text{O}_{7-x}$  observed by  $^{155}\text{Gd}$ -Mossbauer spectroscopy // Solid State Commun. 1990. V. 75. P. 981–985.

**A. V. Nikolaeva, P. P. Seregin, A. B. Jarkoi**

### USING THE $^{57m}\text{Fe}^{3+}$ MÖSSBAUER PROBE TO DETERMINE THE EFG TENSOR PARAMETERS IN THE COOPER SITES TO THE LATTICES OF $\text{CuO}$ And $\text{La}_{2-x}\text{Sr}_x\text{CuO}_4$

*Mössbauer emission spectroscopy of the  $^{57}\text{Co}$ ( $^{57m}\text{Fe}$ ) isotope has shown that the impurity iron atoms appearing at the  $\text{CuO}$ -lattice cation sites after the decay of  $^{57}\text{Co}^{2+}$  are donors and can become stabilized in two charge states,  $^{57m}\text{Fe}^{3+}$  and  $^{57m}\text{Fe}^{2+}$ . A satisfactory agreement between the calculated and experimental values of the quadrupole splitting in Mössbauer spectra has been obtained for the  $^{57m}\text{Fe}^{3+}$  centers. This permits one to consider the results obtained in the  $^{57}\text{Co}$ ( $^{57m}\text{Fe}$ ) Mössbauer emission spectroscopy study of cuprates as reliable experimental data on the lattice electric-field gradient ( lattice EFG) tensor parameters at copper sites. The parameters of the lattice EFG tensor at the copper sites in the  $\text{La}_{2-x}\text{Sr}_x\text{CuO}_4$  lattice (the main component of the EFG tensor  $V_{zz}$  and the asymmetry parameter) were determined experimentally by emission Mössbauer spectroscopy with  $^{57}\text{Co}$ ( $^{57m}\text{Fe}$ ) isotopes. A comparison of the experimental and calculated dependences of  $V_{zz}$  on  $x$  shows that the holes arising from the substitution of  $\text{La}^{3+}$  by  $\text{Sr}^{2+}$  are localized mainly at the oxygen sites in the  $\text{Cu-O}_2$  plane.*

**Keywords:** Mössbauer emission spectroscopy, electric field gradient tensor.

*А. В. Николаева, П. П. Серегин, А. Б. Жаркой*

**ИСПОЛЬЗОВАНИЕ МЕССБАУЭРОВСКОГО ЗОНДА  $^{57m}\text{Fe}^{3+}$   
 ДЛЯ ОПРЕДЕЛЕНИЯ ПАРАМЕТРОВ ТЕНЗОРА ГЭП  
 В УЗЛАХ МЕДИ РЕШЕТОК  $\text{CuO}$  И  $\text{La}_{2-x}\text{Sr}_x\text{CuO}_4$**

*Методом эмиссионной мессбауэровской спектроскопии на изотопе  $^{57}\text{Co} (^{57m}\text{Fe})$  показано, что примесные атомы железа, образующиеся после распада  $^{57}\text{Co}^{2+}$  в катионных узлах решетки  $\text{CuO}$ , являются донорами и могут стабилизироваться в двух зарядовых состояниях  $^{57m}\text{Fe}^{3+}$  и  $^{57m}\text{Fe}^{2+}$ . Для центров  $^{57m}\text{Fe}^{3+}$  получено удовлетворительное согласие расчетных и экспериментальных величин квадрупольного расщепления мессбауэровских спектров. Последнее обстоятельство позволяет рассматривать данные по исследованию металлоксидов меди методом эмиссионной мессбауэровской спектроскопии на изотопе  $^{57}\text{Co} (^{57m}\text{Fe})$  в качестве надежных результатов по экспериментальному определению параметров тензора кристаллического ГЭП в узлах меди. Параметры тензора кристаллического ГЭП в узлах меди в решетке  $\text{La}_{2-x}\text{Sr}_x\text{CuO}_4$  (главная компонента тензора ГЭП  $V_{zz}$  и параметр асимметрии) были экспериментально определены методом эмиссионной мессбауэровской спектроскопии на изотопах  $^{57}\text{Co} (^{57m}\text{Fe})$ . Сравнение экспериментальных и рассчитанных зависимостей  $V_{zz}(x)$  показало, что дырки, возникающие при замещении  $\text{La}^{3+}$  на  $\text{Sr}^{2+}$ , локализуются преимущественно в узлах кислорода в  $\text{Cu-O}_2$  плоскости.*

**Ключевые слова:** эмиссионная мессбауэровская спектроскопия, тензор градиента электрического поля.

**1. Introduction**

The Mössbauer spectroscopy is widely used for investigations of high-temperature superconductors (HTSC) [6; 8]. Because copper does not have Mössbauer isotopes, Mössbauer spectroscopy of  $^{57}\text{Fe}$  impurity atoms is extensively used in investigations of the copper sublattices; it is assumed that the  $^{57}\text{Fe}$  probe stabilizes at the copper sites of the HTSC sublattices, so that, by comparing the measured with calculated quadrupole splittings in Mössbauer spectra, one can draw conclusions on the nature of the local copper-atom environment [2].

The quadrupole splitting can be calculated reliably only for the  $\text{Fe}^{3+}$  probe having a spherically symmetric  $3d^5$  outer electronic shell, where the electric-field gradient (EFG) at the iron nuclei is generated primarily by lattice ions (the crystal-field EFG). However stabilization of  $\text{Fe}^{3+}$  at the sites of divalent copper  $\text{Cu}^{2+}$  (which is the most probable copper state in most HTSCs) should give rise to the formation of centers compensating the difference in charge between the substituting and replaced atoms. The compensating centers can be located near the impurity probe and in this way affect the EFG in a non-obvious way. The validity of the above considerations was buttressed by study of the state of  $^{57}\text{Fe}$  impurity atoms in  $\text{CuO}$  made by Mössbauer absorption spectroscopy [8]; the  $\text{Fe}^{3+}$  impurity atoms were found to substitute for  $\text{Cu}^{2+}$  ions in the  $\text{CuO}$  lattice to form associations of the type  $[\text{Fe}^{3+}-V-\text{Fe}^{3+}]$  ( $V$  is the cation vacancy), and calculation of the EFG tensor parameters at  $^{57}\text{Fe}$  nuclei in such associations turns out to be a difficult problem because of the creation of additional sources of EFG which change appreciably the total EFG.

As will be shown later, however, these problems can be eliminated by using the emission version of Mössbauer spectroscopy [1; 3–5; 7]. We have carried out a comparison of experimental and theoretical quadrupole splittings in  $^{57}\text{Co} (^{57m}\text{Fe})$  Mössbauer emission spectra of  $^{57m}\text{Fe}^{3+}$  impurity ions in copper sites for the  $\text{CuO}$  and  $\text{La}_{2-x}\text{Sr}_x\text{CuO}_4$  lattices.

## 2. Experimentals and Results

### 2.1. Samples and spectroscopy

Copper oxide was obtained by precipitating copper hydroxide from a  $\text{CuSO}_4$  water solution with an alkali, with subsequent annealing of the sediment in an oxygen ambient. Cobalt in the form of  $^{57}\text{CoSO}_4$  was added to a water solution of blue vitriol, with the cobalt concentration in  $\text{CuO}$  not exceeding  $10^{17}\text{cm}^{-3}$ . The experiments were made with samples of  $\text{La}_{2-x}\text{Sr}_x\text{CuO}_4\text{:}^{57}\text{Co}$  ( $x = 0.1, 0.2, 0.3$ , the cobalt concentration  $\sim 10^{15}\text{cm}^{-3}$ ) synthesized by a conventional ceramic technology. The reference samples were monophasic with a  $\text{K}_2\text{NiF}_4$  structure and had  $T_c$  of 25, 37 and 27 K for  $x = 0.1, 0.15$  and  $0.2$  respectively and  $< 4.2$  K for  $x = 0.3$ . The emission Mössbauer spectra have been recorded using  $\text{CuO}\text{:}^{57}\text{Co}$  and  $\text{La}_{2-x}\text{Sr}_x\text{CuO}_4\text{:}^{57}\text{Co}$  sources and  $\text{K}_4\text{Fe}(\text{CN})_6\cdot 3\text{H}_2\text{O}$  absorber with a surface density of  $0.1\text{mg cm}^{-2}$  of  $^{57}\text{Fe}$ . Isomer shifts IS are given relative to  $\alpha\text{-Fe}$ .

The Mössbauer spectra were measured on a CM-2201 spectrometer at temperatures varied from 295 to 5 K. The absorber was  $\text{K}_4\text{Fe}(\text{CN})_6\cdot 3\text{H}_2\text{O}$  with a  $^{57}\text{Fe}$  surface density of  $0.1\text{mg/cm}^2$ .

The lattice EFG tensors at the  $\text{CuO}$  and  $\text{La}_{2-x}\text{Sr}_x\text{CuO}_4$  sites were calculated according to the point charge model. In the general case the measured quadrupole interaction constant  $C$  is a sum of two terms

$$eQU_{zz} = eQ(1 - \gamma)V_{zz} + eQ(1 - R)W_{zz}, \quad (1)$$

where  $V_{zz}$  and  $W_{zz}$  are the principal components of the tensors of the crystal and valence electric field gradients, and  $\gamma$  and  $R$  are the Sternheimer coefficients of the probe atom.

The contribution of the valence electrons to the total electric field gradient tensor can be neglected for the probe  $^{57}\text{Fe}^{3+}$ . Therefore

$$eQU_{zz} \approx eQ(1 - \gamma)V_{zz}. \quad (2)$$

Thus, the experimental data obtained on the parameters of the electric field gradient tensor using the  $^{57}\text{Fe}^{3+}$  probe can be correlated with calculations of these parameters based on an ionic model of the crystal lattice (point charge model).

We calculated the tensors of the crystal electric field gradient at the copper sites of the  $\text{CuO}$  and  $\text{La}_{2-x}\text{Sr}_x\text{CuO}_4$  lattices based on the point-charge model. In so doing, following the X-ray crystallographic data [8], the lattices were represented as a superposition of the following sublattices:  $\text{Cu}_2\text{O}_2$  and  $[\text{La}_{2-x}\text{Sr}_x][\text{Cu}][\text{O}(1)]_2[\text{O}(2)]_2$ .

The components of crystal EFG tensor were calculated using the equations:

$$V_{pp} = \sum_k e_k^* \sum_i \frac{1}{r_{ki}^3} \left[ \frac{3p_{ki}^2}{r_{ki}^2} - 1 \right] = \sum_k e_k^* G_{ppk}, \quad V_{pq} = \sum_k e_k^* \sum_i \frac{3p_{ki}q_{ki}}{r_{ki}^5} = \sum_k e_k^* G_{pqk}, \quad (3)$$

where  $k$  is the sublattice number,  $i$  is the site number within the sublattice,  $p$  and  $q$  are the Cartesian coordinates,  $e_k^*$  is the atomic charges in the  $k$  sublattice,  $r_{ki}$  is the distance of a site with the  $k$  and  $i$  indices from the reference point.

The lattice sums  $G_{ppk}$  and  $G_{pqk}$  were calculated numerically. The summation was carried out within spheres of  $30\text{Å}$  radius.

### 2.2. $\text{CuO}\text{:}^{57}\text{Co}$

If the copper hydroxide was annealed within the  $830\text{-}920^\circ\text{C}$  interval (the anneal time was 2 h), the Mössbauer spectra of  $\text{CuO}\text{:}^{57}\text{Co}$  samples taken at 295 K were a superposition of two quadrupole doublets (fig. 1) with isomer shifts corresponding to the ions  $^{57}\text{Fe}^{3+}$  (spectrum I) and

$^{57m}\text{Fe}^{2+}$  (spectrum 2), with the fraction of the  $^{57m}\text{Fe}^{3+}$  ions being 0.79 (0.02) for the anneal temperature of 920°C, and 0.19 (0.02) for 830°C. The parameters of spectra 1 and 2 are listed in table I. A decrease of the spectrum measurement temperature below the Neel point is accompanied by a broadening of the spectra, with a gradual onset of the allowed hyperfine structure (spectrum 3 in fig. 2). It is significant that, even for a sample containing  $\text{Fe}^{3+}$  and  $\text{Fe}^{2+}$  in a ratio —1:1, the spectrum taken at 5 K was a magnetic sextet corresponding to one iron-atom state only (fig. 2). The characteristics of this spectrum are given in table I. The magnitude of the isomer shift and magnetic field at the nucleus are typical of divalent iron.

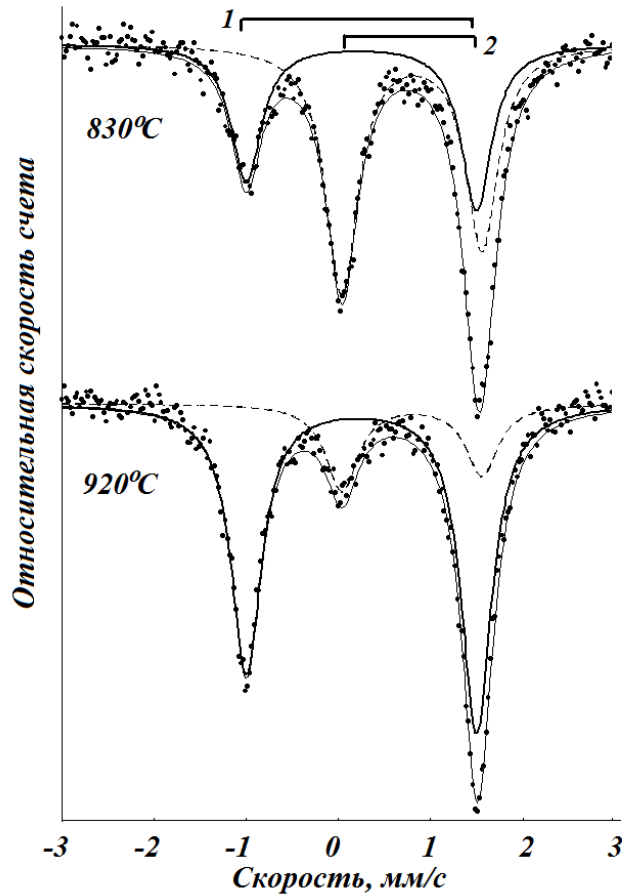


Fig. 1. Mössbauer emission spectra of  $\text{CuO}:\text{}^{57}\text{Co}$  measured at 295 K samples annealed at 920 °C and 860 °C. The experimental spectra are unfolded into quadrupole doublets, and the positions of these doublets corresponding to (1)  $^{57m}\text{Fe}^{3+}$  and (2)  $^{57m}\text{Fe}^{2+}$  centers are shown

Table I

Parameters of the Mössbauer emission spectra of  $^{57m}\text{Fe}$  impurity atoms in  $\text{CuO}$

Type of spectrum	$T$ , K	Ion	$\Delta$ mm/s	$IS$ , mm/s	$G$ , mm/s	$B$ , T
1	295	$\text{Fe}^{3+}$	2.50(2)	-0.25(1)	0.40(2)	
2	295	$\text{Fe}^{2+}$	1.52(2)	-0.80(1)	0.42(2)	
3	80	$\text{Fe}^{2+}$	1.30(4)	-0,81(2)	0.45(3)	25.5(2)

Note.  $\Delta$  — Quadrupole splitting,  $IS$  — isomer shift,  $G$  — spectral linewidth,  $B$  —magnetic-field induction at the  $^{57m}\text{Fe}^{3+}$  nuclei.

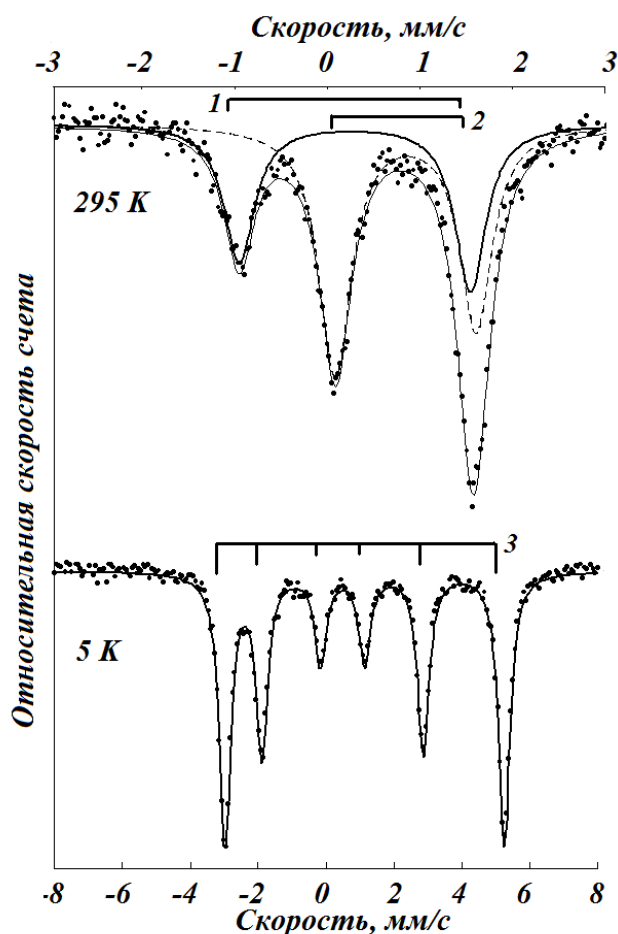


Fig. 2. Mössbauer emission spectra of  $\text{CuO}^{57}\text{Co}$  measured at 295 K and 5 K for a sample annealed at 870 °C (the ratio of the areas bounded by spectra 1 and 2 at 295 K — 0.4:0.6). The 295 K spectrum is deconvoluted into two quadrupole doublets, and the positions of these doublets corresponding to (1)  $^{57m}\text{Fe}^{3+}$  and (2)  $^{57m}\text{Fe}^{2+}$  centers are shown. (3) The position of the components of the Zeeman sextet corresponding to the  $^{57m}\text{Fe}^{2+}$  centers at 5 K

The presence of a correlation between the transition of  $\text{CuO}$  to the antiferromagnetic state and the creation of magnetic fields at the  $^{57m}\text{Fe}$  nuclei permits a conclusion that the impurity cobalt atoms enter copper sites in the  $\text{CuO}$  lattice, and that the daughter  $^{57m}\text{Fe}$  iron atoms produced in the cobalt radioactive decay may reside in different charge states, at least at room temperature.

The chemical properties of cobalt and the conditions of sample preparation used suggest that cobalt impurity atoms should form  $\text{Co}^{2+}$  isovalent substitutional centers in the  $\text{CuO}$  lattice, so that the  $^{57m}\text{Fe}$  daughter atoms should occupy substitutional sites.

It should be pointed out that electron capture in  $^{57}\text{Co}$  is accompanied by Auger-electron emission leaving the daughter atom in a multiply ionized state  $^{57m}\text{Fe}^{n+}$  ( $n \sim 7$ ). Such an ion is an effective trapping center for Auger electrons, and the  $^{57m}\text{Fe}^{n+}$  ion becomes neutralized to one of its valence-stable states in a time  $\sim 10^{-12}$  s. The final stabilized state of the daughter atom ( $^{57m}\text{Fe}^{2+}$  or  $^{57m}\text{Fe}^{3+}$ ) depends, however, both on the nature of the electrical activity of the iron center and on the nature and concentration of electrically active native defects in the  $\text{CuO}$  lattice [1; 2; 5; 10; 11].

EPR data show undoped  $\text{CuO}$  samples to be oxygen deficient, this deficiency being the larger, the higher is the anneal temperature; oxygen deficiency can be reduced by annealing in an oxygen ambient [12]. Thus it could be expected that spectrum 1 is due to single  $^{57m}\text{Fe}^{3+}$  impurity

ions produced by radioactive decay of  $^{57}\text{Co}^{2+}$  in the CuO copper sites. In other words, one of the Auger electrons is captured during the  $^{57m}\text{Fe}^{n+}$  neutralization by a native lattice defect.

We calculated the crystal-field EFG tensor for the cation site in the CuO lattice in the point-charge approximation (the lattice was presented in the  $\text{Cu}^{2+}\text{O}^2$  form). The crystal-field EFG tensor was off-diagonal in the crystallographic axes, and its diagonalization yields  $V_{zz} = 0.738 e/\text{\AA}^3$  and  $\eta = 0.29$ , where  $\eta = (V_{yy} - V_{xx})/V_{zz}$  is the asymmetry parameter of the crystal-field EFG tensor, and  $V_{xx}$ ,  $V_{yy}$ , and  $V_{zz}$  are components of the crystal-field EFG tensor, with  $|V_{zz}| > |V_{yy}| > |V_{xx}|$ .

The quadrupole splitting of a  $^{57m}\text{Fe}^{3+}$  Mössbauer spectrum was calculated from

$$\Delta^{\text{cr}} = \frac{1}{2} |eQV_{zz}| (1 - \gamma) \left( 1 + \frac{\eta^2}{3} \right)^{1/2}, \quad (4)$$

where  $\gamma$  is the Sternheimer coefficient [for the  $\text{Fe}^{3+}$  ion,  $\gamma = -(7.97 - 9.14)$  [8], and the expected value of  $\Delta^{\text{cr}}$  lies from 2.14 to 2.42 mm/s. Thus one observes a satisfactory agreement between the experimental  $\Delta$  and calculated  $\Delta^{\text{cr}}$  quadrupole splittings of Mössbauer spectrum 1, if we assume it to originate from single  $^{57m}\text{Fe}^{3+}$  ions occupying copper sites in the CuO lattice.

The nature of the  $^{57m}\text{Fe}^{2+}$  state presented by spectrum 2 can be understood if one takes into account the experimental observation that the only state left in the emission spectra taken below the Neel temperature of samples containing comparable amounts of  $^{57m}\text{Fe}^{2+}$  and  $^{57m}\text{Fe}^{3+}$  is  $^{57m}\text{Fe}^{2+}$ . Obviously enough the transition of  $^{57m}\text{Fe}^{3+}$  to  $^{57m}\text{Fe}^{2+}$  entails electronic processes. In other words, the  $^{57m}\text{Fe}^{2+}$  ion should be considered as a neutral donor center, whereas  $^{57m}\text{Fe}^{3+}$  is a singly ionized state of this center. The fine structure of a Mössbauer emission spectrum depends on the relative length of the time required for a thermodynamic equilibrium to set in between the neutral and ionized iron centers,  $\tau$ , and the lifetime  $\tau_0$  of the  $^{57}\text{Fe}$  Mössbauer level, namely, if  $\tau \ll \tau_0$ , the experimental spectrum will reflect an averaged state of iron atoms produced in a fast electron exchange between the  $^{57m}\text{Fe}^{2+}$  and  $^{57m}\text{Fe}^{3+}$  centers, while if  $\tau \gg \tau_0$ , the experimental spectrum will be a superposition of the  $^{57m}\text{Fe}^{2+}$  and  $^{57m}\text{Fe}^{3+}$  spectra, and the  $^{57m}\text{Fe}^{3+}$  contribution to the spectrum will correspond to the fraction of the  $^{57}\text{Co}$  atoms having electron trapping centers within the mean free path  $\lambda_0$  of the Auger electrons.

Taking into account the presence of both iron states in room-temperature spectra of  $\text{CuO}^{57}\text{Co}$  samples, one should conclude that the emission spectra of  $\text{CuO}^{57}\text{Co}$  reflect a nonequilibrium situation ( $\tau \gg \tau_0$ ) arising in the course of neutralization of highly-charged  $^{57m}\text{Fe}^{n+}$  states in the CuO lattice, and that the fraction of  $^{57m}\text{Fe}^{3+}$  ions contributing to the spectra corresponds to that of the  $^{57}\text{Co}^{2+}$  atoms having electron trapping centers within their close environment (within  $\lambda_0$ ).

Decreasing the temperature of spectral measurements from 295 to 5 K brings about stabilization of all daughter iron atoms in the  $^{57m}\text{Fe}^{2+}$  neutral state only. To interpret this observation, one should recall that undoped cupric oxide CuO is oxygen deficient and  $n$  type. The isovalent  $^{57}\text{Co}^{2+}$  impurity in the CuO lattice is electrically inactive, and its presence does not affect the Fermi level position. The concentration of electrically active  $^{57m}\text{Fe}$  iron centers in CuO is so low that the presence of iron likewise does not influence the Fermi level. Thus the position of the Fermi level is controlled only by native defects in the CuO structure. At low temperatures, the Fermi level lies close to the conduction-band bottom, and all native-defect levels are occupied by electrons. Therefore the Auger electrons formed in the course of radioactive transformation of the parent  $^{57}\text{Co}^{2+}$  atoms become trapped by the daughter iron atoms, so that all iron atoms end up by being stabilized in the  $^{57m}\text{Fe}^{2+}$  state (with no free-electron-capture centers present within a distance of  $\lambda_0$ ). An increase of temperature shifts, as a rule, the Fermi level towards the midgap and,

therefore, part of the native-defect levels turn out to be free and can act as Auger-electron trapping centers. As a result, iron atoms stabilize in the form of both  $^{57}\text{Fe}^{2+}$  and  $^{57}\text{Fe}^{3+}$ , with the concentration ratio of these forms depending on both the spectrum measurement temperature (the higher the temperature, the larger is the fraction of the  $^{57}\text{Fe}^{3+}$  centers) and the concentration of native defects (other conditions being equal, the native-defect concentration is the higher, the higher is the anneal temperature and, hence, the higher is the  $^{57}\text{Fe}^{3+}$  center concentration).

### 2.3. $\text{La}_{2-x}\text{Sr}_x\text{CuO}_4:^{57}\text{Co}$

The emission Mössbauer spectra of the  $\text{La}_{2-x}\text{Sr}_x\text{CuO}_4:^{57}\text{Co}$  samples are quadrupole doublets, which points to a non-cubic environment of the Cu sites (fig. 3).

The isomer shifts of all spectra correspond to  $\text{Fe}^{3+}$ . The quadrupolar splitting of the  $^{57}\text{Fe}$  Mössbauer spectra is determined by the excited state of the nucleus (spin  $I = 3/2$ , quadrupole moment  $Q = 0.211$  b) and is described as follows

$$\Delta = \frac{1}{2} |eQU_{zz}| \left( 1 + \frac{\eta^2}{3} \right)^{1/2}, \quad (5)$$

where  $U_{zz}$  is the principal component of the total EFG tensor at the  $^{57}\text{Fe}$  nucleus;  $\eta = (U_{xx} - U_{yy})/U_{zz}$  is the asymmetry parameter of the total EFG tensor. For the tensor components the inequality  $U_{xx} \leq |U_{yy}| \leq |U_{zz}|$  should be valid.

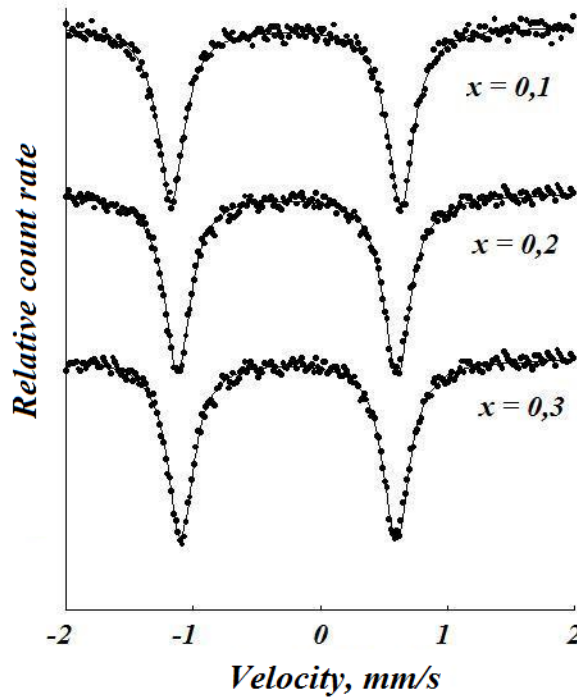


Fig 3. The Mössbauer spectra of  $\text{La}_{2-x}\text{Sr}_x\text{CuO}_4:^{57}\text{Co}$  recorded at 295 K

Thus, the value of  $\Delta$  is proportional to  $|U_{zz}|$ , which is determined by the lattice EFG for the  $\text{Fe}^{3+}$  probe  $U_{zz} \approx (1-\gamma) V_{zz}$ , where  $V_{zz}$  and  $\gamma$  relate to the Cu sites and  $\text{Fe}^{3+}$  ion, respectively.

To identify the compensating centres arising from Sr doping of the  $\text{La}_{2-x}\text{Sr}_x\text{CuO}_4$  lattice, we calculated the EFG tensor components at the copper and lanthanum sites in the framework of the point charge model. According to [8], the atomic positions in the unit cell were:

(La,Sr): (0, 0, 0.36046c), (0, 0, 0.63954c), (a/2, b/2, 0.13954c), (a/2, b/2, 0.86046c);

(Cu): (0, 0, 0), (a/2, b/2, c/2);

O(1): (0, 0, 0.1824c), (0, 0, 0.8176c), (a/2, 6/2, 0.3176c), (a/2, 6/2, 0.6824c);

O(2): (a/2, 0, 0), (0, b/2, 0), (a/2, 0, c/2), (0, b/2, c/2).

The lattice-sum tensors from the individual sub-lattices are diagonal in the crystalline axes and have an axial symmetry ( $\eta = 0$ ). Their principal axes coincide with the  $c$  axis.

In addition, we calculated the principal component of the lattice EFG  $V_{zz} = V_{cc}$  for various combinations of  $\text{La}^{3+}$ ,  $\text{Sr}^{2+}$ ,  $\text{Cu}^{2+}$ ,  $\text{Cu}^{3+}$ ,  $\text{O}^{2-}$  and  $\text{O}^{-}$  ions at the  $\text{La}_{2-x}\text{Sr}_x\text{CuO}_4$  lattice sites using formula (5) and taking into account the electronegativity requirement. If a sublattice included ions with different charges ( $\text{La}^{3+}$  and  $\text{Sr}^{2+}$ ,  $\text{Cu}^{2+}$  and  $\text{Cu}^{3+}$ ,  $\text{O}^{2-}$  and  $\text{O}^{-}$ ), then their total charge was considered as uniformly distributed over all the sites of the sublattice, i.e.,  $e_k^*$  was taken to be equal to the average charge of the sublattice ions. This model is supported by the smooth dependence of the Mössbauer spectral parameters on  $x$ , whereas the charge localization at the sites near the Mössbauer probe would produce additional spectral lines.

The calculated values for  $V_{zz}$  vary from  $0.55 \text{ e}/\text{\AA}^3$  to  $0.70 \text{ e}/\text{\AA}^3$  for  $x = 0.1$  to  $0.3$ . The  $eQU_{zz}$  values determined from the  $^{57}\text{mFe}^{3+}$  Mössbauer spectra are within the range of the calculated values, which seems to indicate a higher reliability of the Sternheimer coefficient for  $\text{Fe}^{3+}$ . But the absolute value of  $eQU_{zz}$  cannot be used to identify the compensating centres. The difference can be accounted for by the uncertainty of the Sternheimer coefficient and by the reduced ion charges as compared with the formal chemical ones (the so-called lattice charge contrast).

However, knowledge of the  $eQU_{zz}$  value is unnecessary, because its relative variation is sufficient to make the identification by comparing the dimensionless parameters  $P = [eQU_{zz}]_x/[eQU_{zz}]_{x=0.1}$  and  $p = [V_{zz}]_x/[V_{zz}]_{x=0.1}$ . It is important that, unlike  $eQU_{zz}$ , the experimental parameter  $P$  depends neither on the Sternheimer coefficient nor on the charge contrast of the lattice. Figure 4 shows the  $p(x)$  plots for copper sites calculated for four possible models: (A) the hole is in the copper sublattice with the average site charge  $(2+x)e$ ; (B) the hole is in the O(1) sublattice with the average O(1) charge  $-2(2-x/2)e$ ; (C) the hole is in the O(2) sublattice with the average O(2) charge  $-(2-x/2)e$ ; (D) the hole is shared by the O(1) and O(2) sublattices with the oxygen charge  $-(2-x/4)e$ .

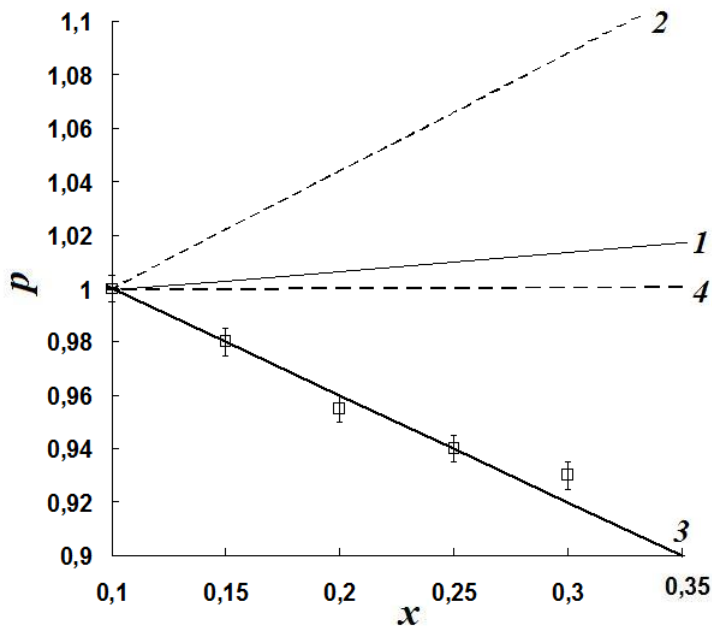


Fig. 4. The  $p - x$  plots for copper sites in  $\text{La}_{2-x}\text{Sr}_x\text{CuO}_4$ . The calculated curves A, B and C are for a hole at the Cu, O(1) and O(2) sublattice and D for a hole shared between the O(1) and O(2) sublattices respectively. The experimental points are related to the  $^{57}\text{mFe}^{3+}$ .



In all of these cases the La(Sr) ion charge was taken as  $(3 - x/2)e$ . The experimental  $P$  points plotted in fig. 4 show that the decrease of  $eQU_{zz}$  with increasing  $x$  for  $^{57m}\text{Fe}^{3+}$  can be described quantitatively only for the holes localized in the O(2) or predominantly in the O(2) sublattice. The other three models contradict the experimental data. The  $P$  values in fig. 3 calculated from the  $^{57}\text{Fe}$  absorption Mössbauer data for the  $\text{La}_{2-x}\text{Sr}_x\text{Cu}_{0.995}\text{Fe}_{0.005}\text{O}_4$  samples [9] show a much stronger dependence on  $x$  than predicted by the calculations. The difference in the behaviour of the  $^{57m}\text{Fe}^{3+}$  and  $^{57}\text{Fe}^{3+}$  centres in the  $\text{La}_{2-x}\text{Sr}_x\text{CuO}_4$  lattice can be attributed to their different origin and local symmetry. The  $^{57m}\text{Fe}^{3+}$  centres arise from  $^{57}\text{Co}^{2+}$  at the regular copper sites, whereas the  $^{57}\text{Fe}^{3+}$  ones, having substituted  $\text{Cu}^{2+}$  in the synthesis, have some compensating centres (like cation vacancies) in their vicinity, which leads to an uncontrolled change in the resulting EFG.

### 3. Conclusion

By the Mössbauer spectroscopy both the isolated  $^{57m}\text{Fe}^{3+}$  centers in the cation sites of the CuO lattice (emission spectroscopy). For the isolated  $^{57m}\text{Fe}^{3+}$  centers a satisfactory agreement has been established between the quadrupole splitting values calculated by the point charge model on the one hand and measured in the Mössbauer spectra on the other hand. This conclusion seems to be valid for copper sublattices of high- $T_c$  superconductors, and should be taken into account in the interpretation of the Mössbauer spectra of Fe-doped HTSCs. The  $^{57}\text{Co}$ ( $^{57m}\text{Fe}$ ) emission spectroscopy is preferable in this aspect.

The comparison of experimental and calculated dependences of the EFG at the cation sites of  $\text{La}_{2-x}\text{Sr}_x\text{CuO}_4$  on the  $x$  value indicates that the compensating centres arising from the substitution of  $\text{La}^{3+}$  by  $\text{Sr}^{2+}$  are the holes totally or predominantly localized in the O(2) sublattice, i.e. at the oxygen sites in the  $\text{CuO}_2$  plane.

### СПИСОК ЛИТЕРАТУРЫ

1. Ефимов А. А., Шунатов В. Т., Серегин П. П. Эффект Мессбауэра на примесных атомах железа в  $\text{Co}_3\text{O}_4$  // Физика твердого тела. 1969. Т. 11. С. 3032–3033.
2. Мастеров В. Ф., Насрединов Ф. С., Серегин Н. П., Серегин П. П. Использование мессбауэровского зонда  $^{57m}\text{Fe}^{3+}$  для определения параметров тензора ГЭП в катионных узлах решетки CuO // Физика твердого тела. 1999. Е. 41. Вып. 8. С.1403–1406.
3. Мастеров В. Ф., Насрединов Ф. С., Саидов Ч. С., Серегин П. П., Бондаревский С. И., Щербатюк О. К. Сверхтонкие взаимодействия в узлах меди решетки  $\text{La}_{2-x}\text{Sr}_x\text{CuO}_4$ , изученные методом эмиссионной мессбауэровской спектроскопии на изотопе  $^{61}\text{Cu}$ ( $^{61}\text{Ni}$ ) // Сверхпроводимость: физика, химия, технология. 1992. Е. 5. Вып. 7. С. 1339–1341.
4. Мастеров В. Ф., Насрединов Ф. С., Серегин П. П., Саидов Ч. С. Экспериментальное определение параметров тензора кристаллического ГЭП в узлах редкоземельных металлов решеток  $\text{R}\text{Ba}_2\text{Cu}_3\text{O}_7$  методом эмиссионной мессбауэровской спектроскопии на изотопе  $^{155}\text{Eu}$ ( $^{155}\text{Gd}$ ) // Сверхпроводимость: физика, химия, технология. 1993. Т. 6. Вып. 3. С. 563–567.
5. Мулин А. Н., Лурье Б. Г., Серегин П. П. Исследование зарядовых состояний железа в окислах кобальта методом Мессбауэра // Физика твердого тела. 1968. Т. 10. Вып. 9. С. 2624–2627.
6. Насрединов Ф. С., Серегин П. П. Исследование состояния примесных атомов олова в окиси никеля методом Мессбауэра // Физика твердого тела. 1973. Т. 15. Вып. 2. С. 385–389.
7. Серегин П. П., Бондаревский С. И., Ефимов А. А. Эффект Мессбауэра на атомах  $^{57m}\text{Fe}$  в  $\text{CoS}$  // Физика твердого тела. 1970. Т. 12. С. 1841–1842.
8. Bordovsky G., Marchenko A., and Seregin P. Mössbauer of Negative Centers in Semiconductors and Superconductors. Identification, Properties, and Application. Academic Publishing GmbH & Co. 2012. 499 p.
9. Imbert P., Jehanno G., Hodges J. A. Mössbauer study of super and semi-conducting samples of  $^{57}\text{Fe}$ -doped  $\text{La}_{2-x}\text{Sr}_x\text{CuO}_4$  // Hyperfine Interact. 1989. V. 50. P. 599–606.
10. Regel' A. R., Seregin P. P. Mössbauer investigations of impurity atoms in semiconductors // Soviet physics. Semiconductors 1984. V. 18. No. 7. P. 723–734.

11. *Seregin P. P., Nasredinov F. S., Vasilev L. N.* A study of radiation defects in solids by means of Mössbauer spectroscopy // *Physica Status Solidi (A) Applied Research*. 1978. V. 45. No. 1. P. 11–45.
12. *Stewart S. J., Borzi R.A., Punte G., Mereader R. C.* Phase stability and magnetic behavior of Fe-doped CuO // *Phys. Rev. B*. 1998. V. 57. P. 4983–4986.

## REFERENCES

1. *Efimov A. A., Shipatov V. T., Seregin P. P.* Effekt Messbaujera na primesnyh atomah zheleza v  $\text{So}_3\text{O}_4$  // *Fizika tverdogo tela*. 1969. T. 11. S. 3032–3033.
2. *Masterov V. F., Nasredinov F. S., Seregin N. P., Seregin P. P.* Ispol'zovanie messbaujеровского zonda  $^{57}\text{mFe}^{3+}$  dlja opredelenija parametrov tenzora GEP v kationnyh uzlah reshetki CuO // *Fizika tverdogo tela*. 1999. T. 41. Vyp. 8. S.1403–1406.
3. *Masterov V. F., Nasredinov F. S., Saidov Shch. S., Seregin P. P., Bondarevskij S. I., Werbatjuk O. K.* Sverhtonkie vzaimodejstvija v uzlah medi reshetki  $\text{La}_{2-x}\text{Sr}_x\text{CuO}_4$ , izuchennye metodom emissionnoj messbaujеровской spektroskopii na izotope  $^{61}\text{Cu}$ ( $^{61}\text{Ni}$ ) // *Sverhprovodimost': fizika, himija, tehnologija*. 1992. T. 5. Vyp. 7. S. 1339–1341.
4. *Masterov V. F., Nasredinov F. S., Seregin P. P., Saidov Shch. S.* Eksperimental'noe opredelenie parametrov tenzora kristallicheskogo GEP v uzlah redkozemel'nyh metallov reshetok  $\text{RBa}_2\text{Cu}_3\text{O}_7$  metodom emissionnoj messbaujеровской spektroskopii na izotope  $^{155}\text{Eu}$ ( $^{155}\text{Gd}$ ) // *Sverhprovodimost': fizika, himija, tehnologija*. 1993. T. 6. Vyp. 3. S. 563–567.
5. *Murin A. N., Lur'e B. G., Seregin P. P.* Issledovanie zarjadovyh sostojanij zheleza v oksilah kobal'ta metodom Messbaujera // *Fizika tverdogo tela*. 1968. T. 10. Vyp. 9. S. 2624–2627.
6. *Nasredinov F. S., Seregin P. P.* Issledovanie sostojanija primesnyh atomov olova v okisi nikelja metodom Messbaujera // *Fizika tverdogo tela*. 1973. T. 15. Vyp. 2. S. 385–389.
7. *Seregin P. P., Bondarevskij S. I., Efimov A. A.* Effekt Messbaujera na atomah  $^{57}\text{mFe}$  v CoS // *Fizika tverdogo tela*. 1970. T. 12. S. 1841–1842.
8. *Bordovsky G., Marchenko A., and Seregin P.* Mössbauer of Negative Tsenters in Semiconductors and Superconductors. Identification, Properties, and Applicaton. Academic Publishing GmbH & Co. 2012. 499 p.
9. *Imbert P., Jehanno G., Hodges J. A.* Mössbauer study of super and semiconducting samples of  $^{57}\text{Fe}$ -doped  $\text{La}_{2-x}\text{Sr}_x\text{CuO}_4$  // *Hyperfine Interact.* 1989. V. 50. P. 599–606.
10. *Regel' A. R., Seregin P. P.* Mössbauer investigations of impurity atoms in semiconductors // *Soviet physics. Semiconductors* 1984. V. 18. No. 7. P. 723–734.
11. *Seregin P. P., Nasredinov F. S., Vasilev L. N.* A study of radiation defects in solids by means of Mössbauer spectroscopy // *Physica Status Solidi (A) Applied Research*. 1978. V. 45. No. 1. P. 11–45.
12. *Stewart S. J., Borzi R. A., Punte G., Mereader R. C.* Phase stability and magnetic behavior of Fe-doped CuO // *Phys. Rev. B*. 1998. V. 57. P. 4983–4986.

*М. А. Горяев, А. П. Смирнов*

## ГАЛОГЕНИДЫ СЕРЕБРА КАК УНИКАЛЬНЫЕ ФОТОХИМИЧЕСКИ ЧУВСТВИТЕЛЬНЫЕ ПОЛУПРОВОДНИКИ

*Рассмотрены механизмы и особенности фотохимических процессов в галогенидах серебра, а также основные их свойства. Показано, что зонная структура полупроводника, широкие возможности его легирования, относительно высокая концентрация межузельных ионов серебра, эффективное образование собственных дефектов при электронном фотовозбуждении представляют такое сочетание свойств галогенидов серебра, которое обеспечивает уникальную фотохимическую чувствительность материалов на их основе.*

**Ключевые слова:** бромид и хлорид серебра, зонная структура полупроводника, электрон-ионный механизм фотолиза, образование собственных дефектов.